energies

MDPI

Article

# Analysis of Shallow Subsurface Geological Structures and Ground Effective Thermal Conductivity for the Evaluation of Ground-Source Heat Pump System Installation in the Aizu Basin, Northeast Japan

**Takeshi Ishihara [1,*], Gaurav Shrestha [1], Shohei Kaneko [2] and Youhei Uchida [1]**

[1] Renewable Energy Research Center, Fukushima Renewable Energy Institute, AIST, 2-2-9 Machiikedai, Koriyama, Fukushima 963-0298, Japan; shrestha-g@aist.go.jp (G.S.); uchida-y@aist.go.jp (Y.U.)
[2] Graduate School of Symbiotic Systems Science and Technology, Fukushima University, 1 Kanayagawa, Fukushima, Fukushima 960-1296, Japan; s1671002@ipc.fukushima-u.ac.jp
* Correspondence: t84-ishihara@aist.go.jp; Tel.: +81-29-861-5290

Received: 25 July 2018; Accepted: 10 August 2018; Published: 13 August 2018


**Abstract:** Shallow subsurface geological structure mapping combined with ground effective thermal conductivity values at the basin scale provide an appropriate method to evaluate the installation potential of ground-source heat pump systems. This study analyzed the geological structure of the Aizu Basin (Northeast Japan) using sedimentary cores and boring log and mapped the distribution of average ground effective thermal conductivity in the range from −10 m to −100 m depth calculated from cores and logs. Gravel layers dominate in alluvial fans of the northern and southern basin areas, which are found to be associated with higher average ground effective thermal conductivity values, 1.3–1.4 W/m/K, while central and western floodplain areas show lower values of 1.0–1.3 W/m/K due to the existence of thick mud layers in the shallow subsurface. The results indicate that the conventional closed-loop systems are more feasible in northern and southern basin areas than in the central and western areas. Evaluation for the installation potential of the ground-source heat pump systems using depth-based distribution maps of average ground effective thermal conductivity is the originality of this study. This approach is valuable and proper for the simple assessment of the system installation in different sedimentary plains and basins in Japan and other countries.

**Keywords:** ground-source heat pump system; ground effective thermal conductivity; Quaternary geological structure; Aizu Basin

## 1. Introduction

Ground-source heat pump (GSHP) systems have attracted international attention as one of the most energy-efficient systems for providing space-heating/cooling, snow-melting, hot water supply, and more [1,2]. The installation of GSHP systems has increased worldwide especially in the United States, Europe, and China [3]. In Japan, GSHP systems also have installed increasingly since the year around 2000. The most popular GSHP system in Japan (87%) is the closed-loop system using ground heat exchangers (GHEs) while open-loop and a combination of both systems constitute 12% and 1%, respectively [4]. However, the number of installations in Japan remains limited when compared with the other named countries due largely to uncertainties regarding subsurface information (e.g., geology, groundwater flow, and thermal temperatures) that is required to plan optimal GSHP systems as well as the higher drilling costs associated with GHEs. The heat exchange rates of GHEs are strongly influenced by the ground effective thermal conductivity (i.e., geological structure) and heat advection

by groundwater flow. A suitability assessment based on local hydrogeological information is, therefore, required for the installation development of GSHP systems [5].

Many large Japanese cities are located on alluvial plains and basins that are filled by Quaternary systems. These systems consist of unconsolidated sediments (i.e., gravels, sands, muds, and volcanic materials) deposited during the Quaternary Period (from ca. 2.60 million years ago to the present) and their sedimentary structures are complex and variable for each plain or basin. Gravelly and sandy Quaternary systems also have a high value of hydraulic conductivity and act as suitable aquifers. In regions of geological heterogeneity, the length of GHEs should depend on the distribution depth of preferable layers with a high heat exchange capacity (i.e., aquifers) [6]. Analysis of the geological structure (e.g., distribution and thickness of gravel layers) at the basin scales is, therefore, vital for assessing the installation potential of GSHP systems.

Recent studies regarding the installation suitability of GSHP systems (closed-loop systems) in plain and basin scales have been conducted in several areas of Japan [1,5,7–11]. These works evaluated the installation suitability of GSHP systems on the analytical basis of 3D groundwater flow and heat transport models and illustrated suitability maps (e.g., distribution of appropriate places or heat exchange rates). Computed values of these numerical models were verified against measured filed data (e.g., hydraulic heads, subsurface thermal temperatures, and results of thermal response tests). Fujii et al. [1] and Yoshioka et al. [7] calculated heat exchange rates and illustrated the suitability maps showing the variation of them in the Saga Fukui plains, respectively. Uchida et al. [5] and Nomoto et al. [8] mapped the distribution of appropriate places for GSHP system installation using numerical analysis and hydrogeological field data in the Fukui and Kumamoto plain, respectively. Shrestha et al. [9] prepared the distribution maps of effective thermal conductivity and subsurface temperature based on the results of groundwater flow analysis and field data obtained from thermal response tests in the Tsugaru Plain. Shrestha et al. [10] mapped the distribution of groundwater upflowing areas to estimate appropriate areas for GSHP systems utilizing an artesian (flowing) well in the Aizu Basin. Shrestha et al. [11] showed suitable maps of both a conventional closed-loop systems and a GSHP systems using an artesian well by Shrestha et al. in the same basin [10].

These previous studies assessed the GSHP installation potential based on groundwater flow and heat transport analysis. However, analysis of a detailed geological structure using field data (e.g., sedimentary cores and/or boring log data) has not been conducted sufficiently in these works. Uchida et al. [5] and Nomoto et al. [8] used the thickness of aquifers to evaluate the suitability of GSHP installation. With regard to GSHP installation suitability using geological information, Hamada et al. [12] calculated the average ground effective thermal conductivities from boring log data by length-weighted average methods and mapped their distributions in several areas in Hokkaido. Takemura et al. [13] applied a similar approach and considered the relationship between the average ground as effective thermal conductivity and geological conditions in a 5 $km^2$ area of Setagaya City, Tokyo. In these studies, literature values were used for thermal conductivities of solids. Sakata et al. [14] calculated the thermal conductivities of each lithofacies and the average ground effective thermal conductivity values by probability-weighted average methods and mapped their distribution around Sapporo, Hokkaido. Hamamoto et al. [15] evaluated the distribution of installation potential using existing subsurface geological model in the southeastern part of Saitama Prefecture. However, these studies investigated only limited areas and no studies calculating the distribution of thermal properties at the basin scale have been performed. Moreover, the relationship between ground effective thermal conductivity and detailed geological structures has only been briefly discussed. These existing distribution maps show only a single depth (e.g., 50 or 100 m), which suggests that heterogeneous geological structure (e.g., depth and thickness of gravel layers) cannot be reflected sufficiently in the maps.

The geological structure including the thickness of gravel/mud layers and the three-dimensional continuity of each layer controls the ground effective thermal conductivity as well as the hydrogeological characteristics. Information of the geological structure can be a basic assessment index

for the planning of GSHP systems. For instance, a geological cross-section displays the thickness and distribution depths of gravel layers (i.e., an aquifer with higher effective thermal conductivity) and aids the decision-making process regarding GHE depths. Additionally, the distribution of ground effective thermal conductivity can be essential input data for the analysis of groundwater flow and heat transport. Since the population concentrates in the alluvial plain and basin with geological complexity in Japan, it is important to evaluate its installation potential reflecting heterogeneous geological structure for the installation promotion of the GSHP system.

The purpose of this study is to illustrate a suitability map reflecting a geological structure that enables simple assessment of the installation potential of a GSHP system (conventional closed-loop system). As the target area, the Aizu Basin in Northeast Japan was selected (Figure 1). Several cities and towns are located in the basin including Aizu-Wakamatsu and Kitakata. The average monthly temperature in Aizu-Wakamatsu is about 25 °C in August and −0.6 °C in January with a high amount of snowfall [16]. Heat demand in the basin using a GSHP system for air conditioning and snow melting is, therefore, expected to be high. The cities of Aizu-Wakamatsu and Kitakata promote the use of renewable energy including GSHP systems in administrative policies [17,18], but GSHP systems have not yet been installed.

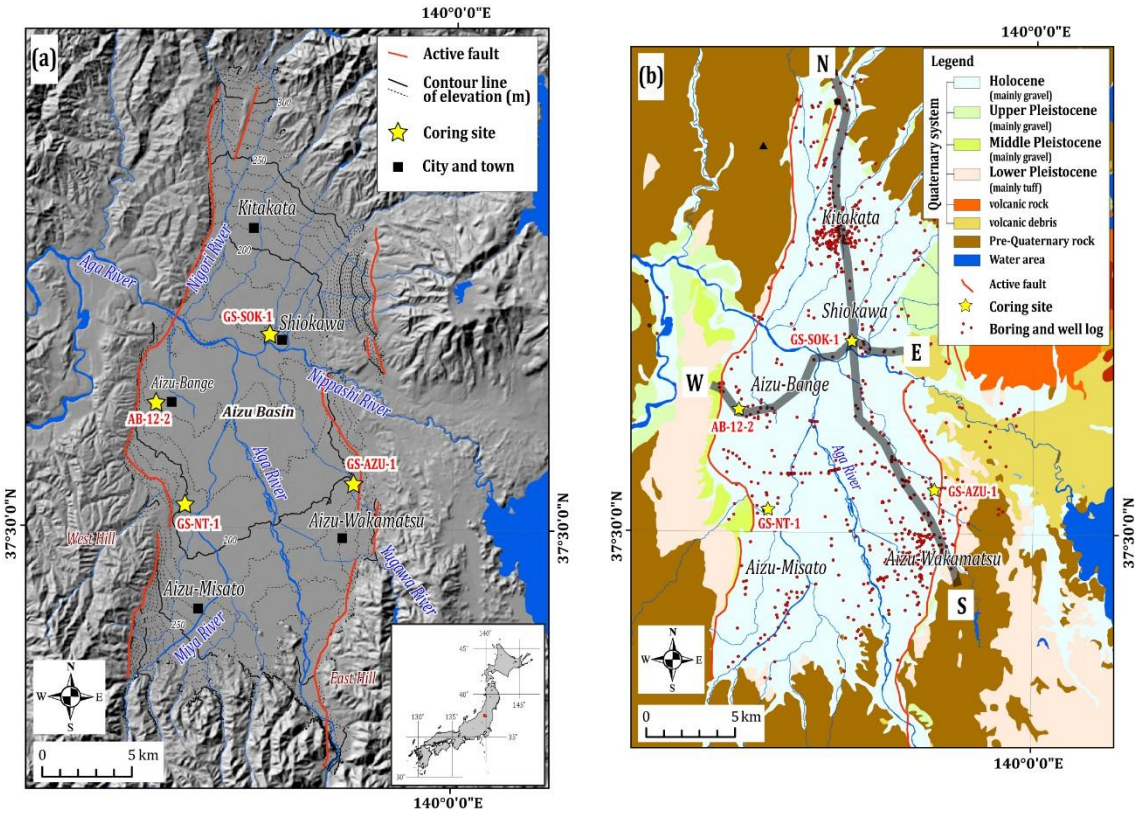


**Figure 1.** (**a**) Location and geography of the Aizu Basin. Relief map and elevation contour lines are drawn from the 50 m grid digital elevation map of the Geospatial Information Authority of Japan (GSI). The contour line interval is 10 m. The distribution of active faults is after Ikeda et al. [19] (**b**) Geological map of the Aizu Basin modified from the geological survey of Japan [20]. Yellow stars represent drilling sites of sedimentary cores shown in Figure 2. N-S and W-E lines represent the location of cross-sections shown in Figures 3 and 4.

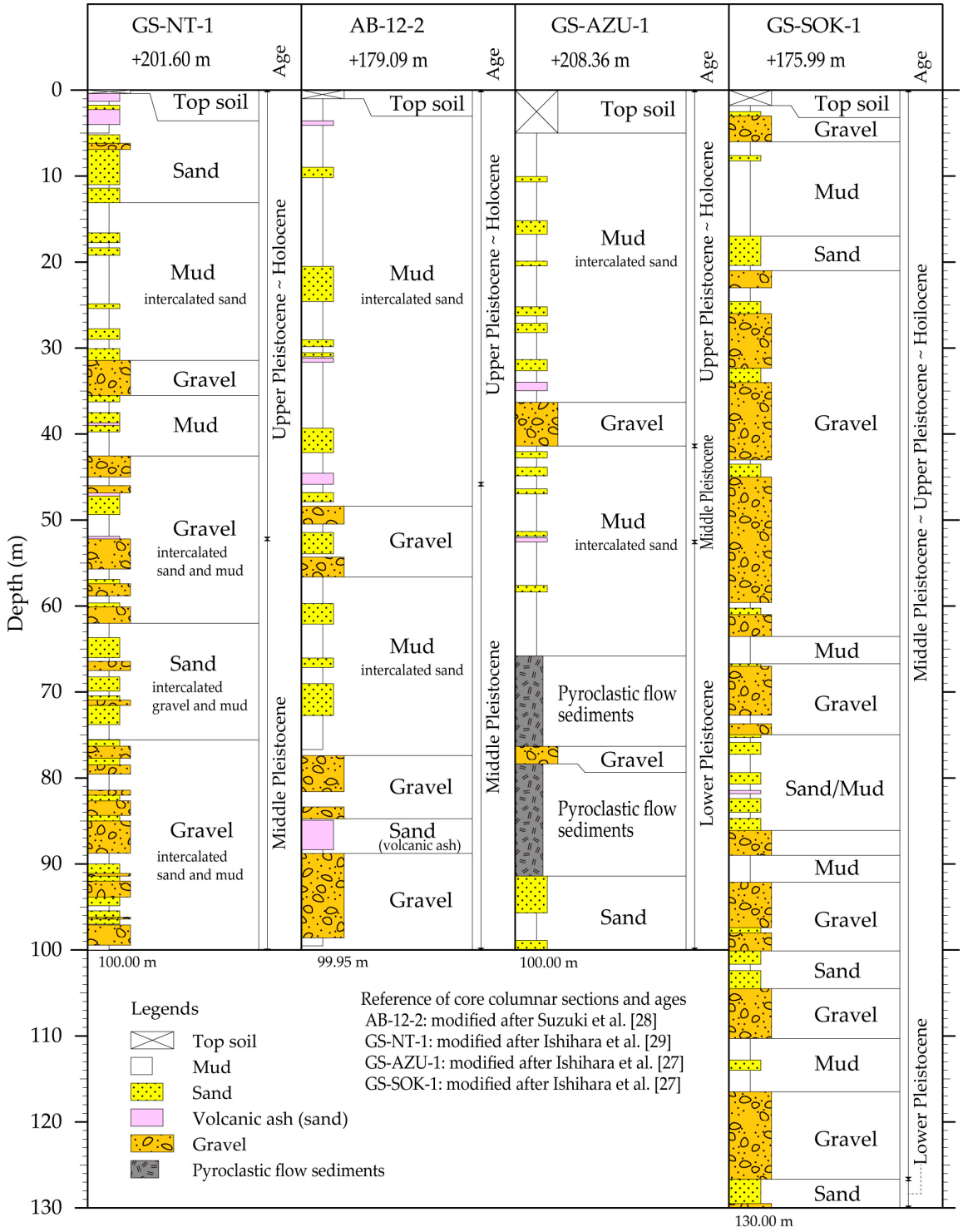


**Figure 2.** Stratigraphic columns of cores drilled in the Aizu Basin. Drilling sites are shown in Figure 1.

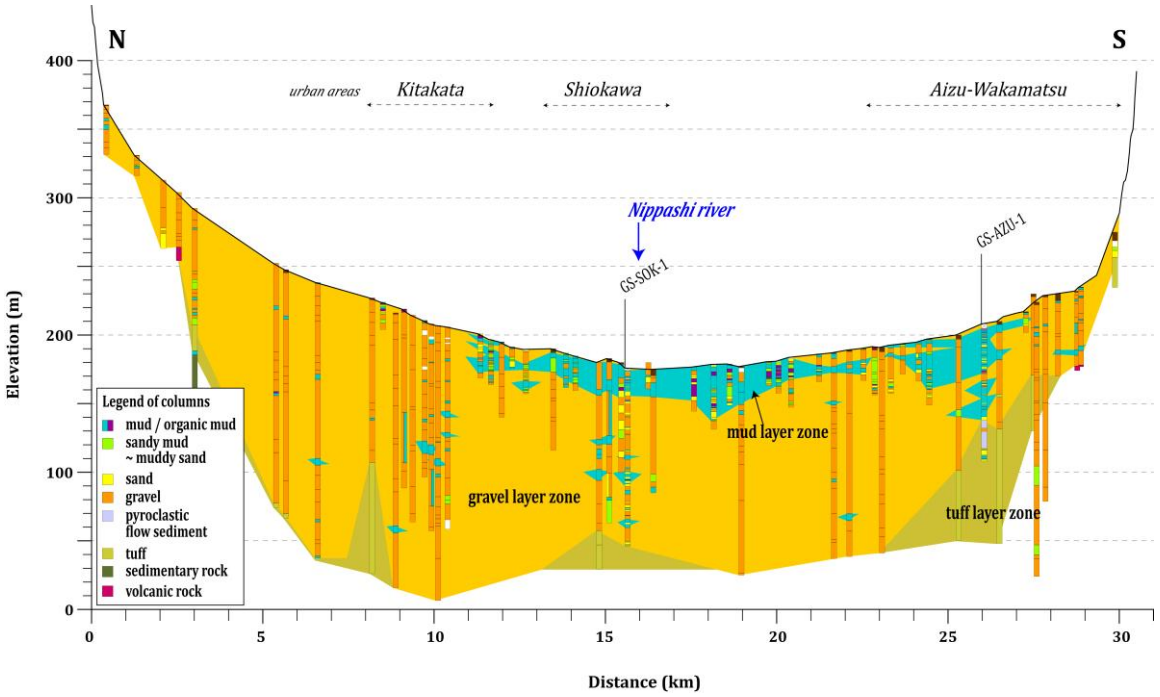


**Figure 3.** N-S cross section shown in Figure 1b. Columns show sedimentary cores, boring, and snow melting well logs.

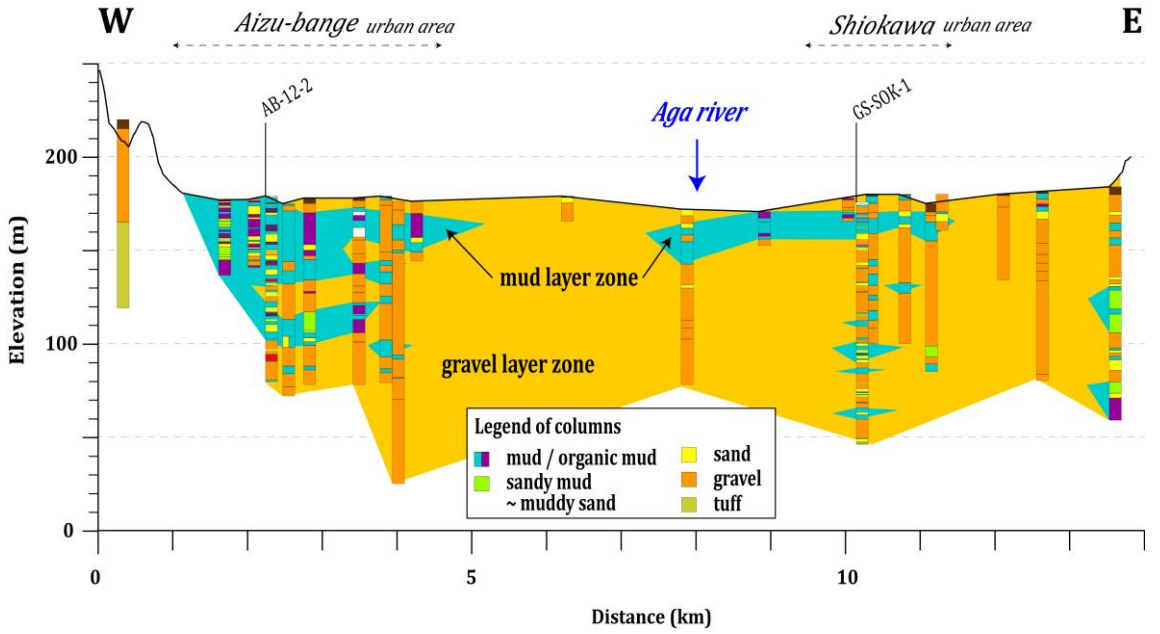


**Figure 4.** W-E cross section shown in Figure 1b. Columns show sedimentary cores, boring, and snow melting well logs.

First, the shallow geological structure up to ca. 100 m depth in the Aizu Basin was reconstructed based on the analysis of sedimentary cores, boring, and snow-melting well logs. The average ground effective thermal conductivity of each log was then calculated and its distribution maps by depth were prepared for basic assessment of the GSHP system. Average ground thermal conductivity values remained relatively high in the northern and southern areas where the gravel layer is dominant while relatively low values were estimated in the central and western areas where thick mud layers distribute

widely in the shallow subsurface. It was found that the conventional closed-loop GSHP systems are more appropriate in the northern and southern areas.

In the distribution maps by depth, the changes of the geological faces in the depth direction were reflected in the distribution of ground effective thermal conductivity values, which indicates that the distribution maps by depth can express the geological structure indirectly. In this way, the suitability evaluation of the GSHP system installation using a ground effective thermal conductivity distribution by depth based on detailed geological structure is the originality of this study. This approach is valuable and proper for simple assessment of the GSHP system when installing in different sedimentary plains and basins in Japan and other countries.

## 2. Study Area

The Aizu Basin lays in the southern part of Northeast Japan and extends N–S for about 32 km and W–E for about 13 km (Figure 1) [21]. The basin is enclosed by mountains in the northern and southern margins consisting of Cretaceous to Paleogene base rocks and Miocene-Pliocene volcanic or sedimentary rocks with an elevation ranging from 1000 m to 2000 m [21,22]. Hills composed of Pliocene to middle Pleistocene sediments exist in the east and the west of the basin with an elevation ranging from 300 m to 800 m [22,23]. Active faults stretch in the N–S direction along the west and east margins [19].

In the Aizu Basin, the Aga River flows northwestward from the southern mountains and runs out from the west of the basin. Tributaries such as the Nippashi, Yugawa, Miya, and Nigori rivers join the Aga River in the central part of the basin. Basin elevations are ca. 170 m in the central-western area, ca. 330 m in the northern margin, and ca. 250 m in the southern margin. As a whole, the basin takes the form of a ship bottom tilting slightly westward. The average gradients along the Aga River are ca. 5/1000 in the southern area and 2/1000 to 3/1000 in the central area of the basin. The average gradients of the eastern and western marginal areas such as Aizu-Wakamatsu and Aizu-Misato are about 10/1000 to 20/1000. The northern area of the basin (Kitakata) has an average gradient of 10/1000 to 15/1000. Alluvial fans formed by the above rivers are distributed in the northern and southern areas as well as the western and eastern margins where the average gradients are steeper. In contrast, a floodplain of the Aga River spread in the central area of the basin with 2/1000 to 3/1000 average gradients.

The Aizu Basin is filled by a Quaternary system consisting of gravels, sands, muds, and tuffs. Its total thickness is over 150 m [21]. However, minimal survey work with detailed geological structural information such as the continuity of mud layers has been reported. Gravel layers of the system host the main basin aquifers where groundwater flow primarily occurs. The groundwater level of the basin lies below 0 m to 5 m from the ground surface [24]. The groundwater level fluctuation ranges observed at nine existing shallow wells in the basin were less than 5 m in most wells [25]. Groundwater recharges at the alluvial fan of the basin margin and flows to the central area of the basin [26]. In the central area, upward flow of groundwater and a muddy confining layer creates an artesian zone [10,11].

## 3. Material and Methods

### *3.1. Analysis of Shallow Subsurface Geological Structure*

In order to reconstruct the shallow subsurface geological structure of the Aizu Basin, we first analyzed four sedimentary core samples (GS-AZU-1, GS-SOK-1, GS-NT-1, and AB-12-2 shown in Figure 1) that were drilled in the basin [27–29]. The depths of each core range from 99.95 to 130.00 m. Additionally, lithofacies data from 790 boring and snow melting well logs were collected. The stratigraphy of these logs was interpreted in terms of the stratigraphic framework of the cores. Several geologic cross-sections were then drawn to clarify the three-dimensional continuity of the gravel and mud layers. Based on these analyses, the geological facies of the basin Quaternary system

were classified into seven types including gravel, sand, mud (mainly silt), peat, tuff (including pyroclastic flow sediment), base rock, and top soil (Table 1).

**Table 1.** Physical parameters of geological facies in the Aizu Basin. Geological facies were re-categorized from Shrestha et al. [10,11]. Porosity and thermal conductivity after Shrestha et al. [10,11].

| Geological Facies | Porosity | Thermal Conductivity (W/m/K) | Ground Effective Thermal Conductivity (W/m/K) | |
|---|---|---|---|---|
| | | | Saturated | Unsaturated |
| Top soil | 0.2 | 1.4 | 1.25 | 1.12 |
| Mud (Silt) | 0.4 | 1.4 | 1.10 | 0.85 |
| Sand | 0.35 | 1.5 | 1.20 | 0.98 |
| Gravel | 0.25 | 1.6 | 1.36 | 1.21 |
| Peat | 0.5 | 0.7 | 0.68 | 0.36 |
| Tuff (Pyroclastic flow sediments) | 0.2 | 1.0 | 0.93 | 0.80 |
| Rock | 0.15 | 2.5 | 2.22 | - |
| Water | - | 0.65 | - | - |
| Air | - | 0.024 | - | - |

### 3.2. Calculation and Mapping of Ground Effective Thermal Conductivity

Table 1 is a list of physical parameters of each classified geological facies in the Aizu Basin. Parameters of porosity and thermal conductivity of each facies were assigned by Shrestha et al. [10,11] who developed a regional-scale 3D groundwater and heat transport model of the basin by using a FEFLOW software package [30] and verified the computed vertical subsurface temperature profiles and hydraulic heads with measured field data. Thermal conductivity and porosity values were determined by a trial-and-error based on a comparison of the above computed and measured values [10,11]. Values of ground effective thermal conductivity obtained parameters of Table 1 are, therefore, representative the basin thermal regime. Ground effective thermal conductivity was calculated using these parameters (see next section). In this calculation, the groundwater level was set to 5 m below the surface. The groundwater level of the basin exists below 0 m to 5 m from the ground surface. The fluctuation ranges were less than 5 m [24]. Even the lowest groundwater level did not fall below 5 m from the ground surface in most shallow wells [25]. This study, therefore, obtains conservatively calculated ground effective thermal conductivity values.

After calculation, distributions of average ground effective thermal conductivity were mapped in the range from a −10 m to −100 m depth using an inverse distance weighted algorithm in the ArcGIS software package (ESRI Japan Corporation).

## 4. Mathematical Formulation

Based on effective thermal conductivity, this study adopts the thermal conductivity and porosity of each classified geological facies used in 3D groundwater flow and heat transport analysis by FEFLOW software [10,11]. In the analysis of FEFLOW, the effective thermal conductivity ($\lambda_g$) of porous media are obtained as below [30,31].

$$\lambda_g = (1 - e)\lambda_s + e\lambda_f \quad (1)$$

where $\lambda_s$ and $\lambda_f$ are the thermal conductivity of the solid (soil/rock) and fluid (water), respectively, and $e$ is the porosity. In this study, due to the consideration of unsaturated layers, Equation (1) was modified as follows [32]:

$$\lambda_g = (1 - e)\lambda_s + eS\lambda_f + e(1 - S)\lambda_a \quad (2)$$

where $\lambda_a$ is the thermal conductivity of air and S is the moisture saturation.

In the case where the ground effective thermal conductivity (average value) of certain location is obtained from boring log data in the plains or basins with geological heterogeneity, the values are

estimated by length-weighted average methods using an effective thermal conductivity and thickness of each facies [13,14].

$$\lambda_{ave} = \Sigma(\lambda_{gk} \times L_k)/\Sigma L_k \quad (3)$$

where $\lambda_{gk}$ and $L_k$ are the thermal conductivity and total thickness of each facies, respectively.

## 5. Results

### *5.1. Shallow Subsurface Geological Structure*

Figure 2 shows stratigraphic columns from four core samples. These columns illustrate that the shallow subsurface stratigraphy of the Aizu Basin is composed of gravel, sand, and mud strata. Pyroclastic flow sediments are found only in the GS-AZU-1 core located in the eastern margin of the basin. Occasional peat layers are also observed in some cores. The age of the core sediments was determined based on the chronological analyses including tephras (volcanic ashes and pyroclastic flow sediments) and radiocarbon dating [27–29]. All strata consist of Quaternary systems including the middle Pleistocene, upper Pleistocene, and Holocene. The lower Pleistocene is composed of pyroclastic flow sediment, gravel, sand, and mud layers and are found in only two cores in the eastern basin area. The middle Pleistocene consists mainly of gravel layers with intercalated sand and mud beds even though thick mud layers are found in the GS-AZU-1 and AB-12-2 cores. Thickness and distribution of intercalated sand/mud layers vary for each core, which indicates that these layers exist locally with poor continuity. In the upper Pleistocene and Holocene, mud layers are relatively dominant. Previous results of tephra analyses and radiocarbon dating indicate that thick mud layers from ca. 5 m to 20–50 m depth in each core were deposited during the same period [27–29].

Representative N–S and W–E geological cross sections are shown in Figures 3 and 4, respectively. The lateral continuity of mud layers was examined in each cross-section based on a comparison between facies of cores and log data. Both sections show that gravel layers are dominant up to 100 m depth from the ground surface throughout the Aizu Basin especially in the northern (Kitakata) and southern regions (Aizu-Wakamatsu and Aizu-Takada). Mud beds are intercalated between gravel layers with a few-meter thickness in the northern and southern areas. However, their lateral continuity appears poor because the distribution depth and thickness vary in each log.

However, thick mud layers exist up to 20 m to 50 m depth from the surface in many boring and well logs from the central and western basin areas, Shiokawa, Aizu-Bange, and the eastern part of Aizu-Wakamatsu (around GS-AZU-1 core site) (Figures 3 and 4). These layers match the core data, which indicates a shallow-depth distribution over the central floodplain areas except a region along the Aga River. Gravel sediments become dominant below 40 m depth around Shiokawa while mud sediments extend below 50 m around Aizu-Bange.

Tuff layers are also found in the deepest part of the well logs from several regions (Figure 3). Core analyses indicate that these layers mainly correlate to pyroclastic flow sediments of the lower Pleistocene [27]. The tuff layers are distributed around 50 m depth in the eastern margin of the southern area and more than 100 m depth in other areas of the basin.

Figure 5a,b illustrate the distribution of the ratio of gravel and mud layers, respectively, up to 50 m depth, which is mapped from core and log data using an inverse distance weighted algorithm in the ArcGIS. Even though local high/low ratios of mud layers exist in the maps due to the distribution bias of the boring log data, the overall trend of the geological structure characteristics is similar to that demonstrated by the cross-sections. The ratio of gravel layers is over 80% (red zone in Figure 5a) in the northern and southern areas of the basin. These gravel-dominant regions correspond to alluvial fan regions with a steep surface gradient, 5–20/1000, formed by the Aga River and its tributaries. By contrast, the ratio of mud layers is about 40–60% (orange and red zones in Figure 5b) in the central and western areas where floodplains with a moderate surface gradient (2–3/1000) are found. Additionally, gravel layers are dominant along the entire Aga River.

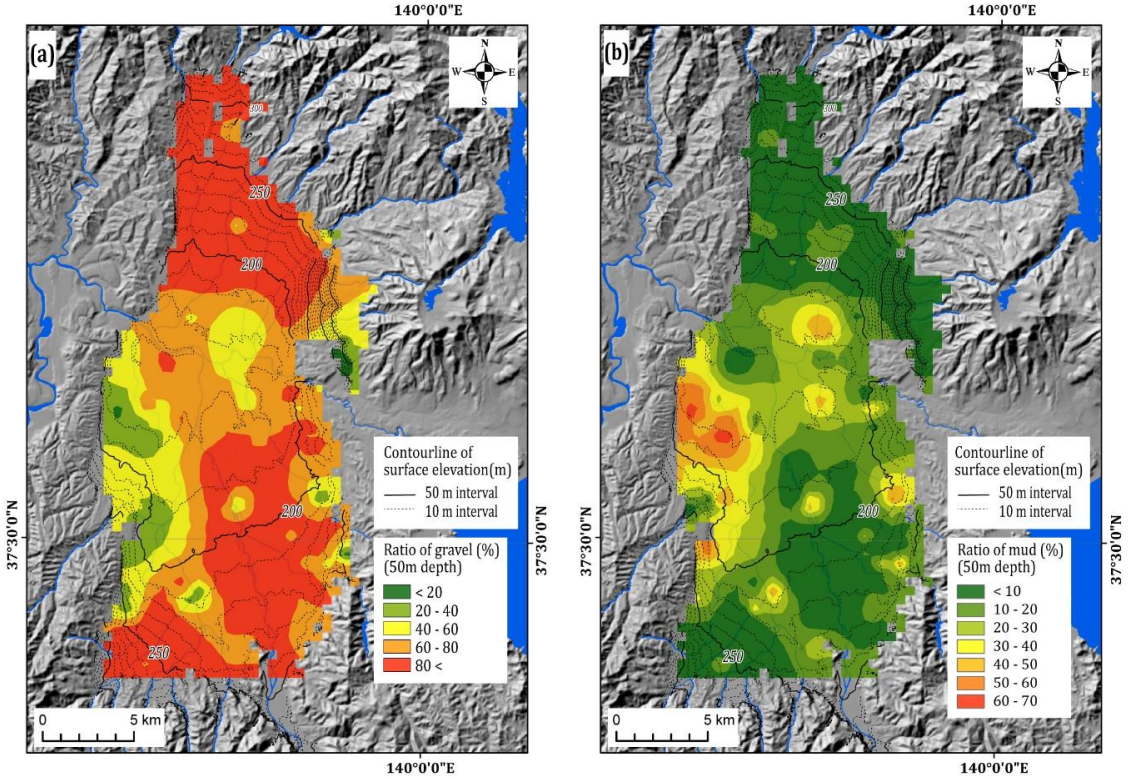


**Figure 5.** Ratio of (**a**) gravel and (**b**) mud layer up to 50 m depth. Relief map and elevation contour lines are drawn from the 50 m grid digital elevation map of the Geospatial Information Authority of Japan (GSI).

### *5.2. Ground Effective Thermal Conductivity Distribution Map*

Figure 6 illustrate the distribution of average ground effective thermal conductivity in the range from −10 m to −100 m depth in the Aizu Basin. Values of the average ground provide effective thermal conductivity ranging from approximately 1.0 W/m/K to 1.7 W/m/K. These values in the −10 m depth map tend to be low throughout the entire basin since the upper half is an unsaturated zone, which decrease values by 4–11% compared with the case of total saturation at the −10 m depth. At −50 m and −100 m depth, these values decrease by 1–2% and <1%, respectively, when compared to the case of total saturation at the same depth.

Values of the average ground and effective thermal conductivity are relatively high in the northern and southern basin areas, 1.3–1.4 W/m/K, and ranged from −20 m to −100 m depth. In the central and western areas, the average ground effective thermal conductivity shows lower values, which are approximately 1.0–1.3 W/m/K, but it tends to increase with depth. In the eastern margin of the basin, these values tend to be lower in the depth.

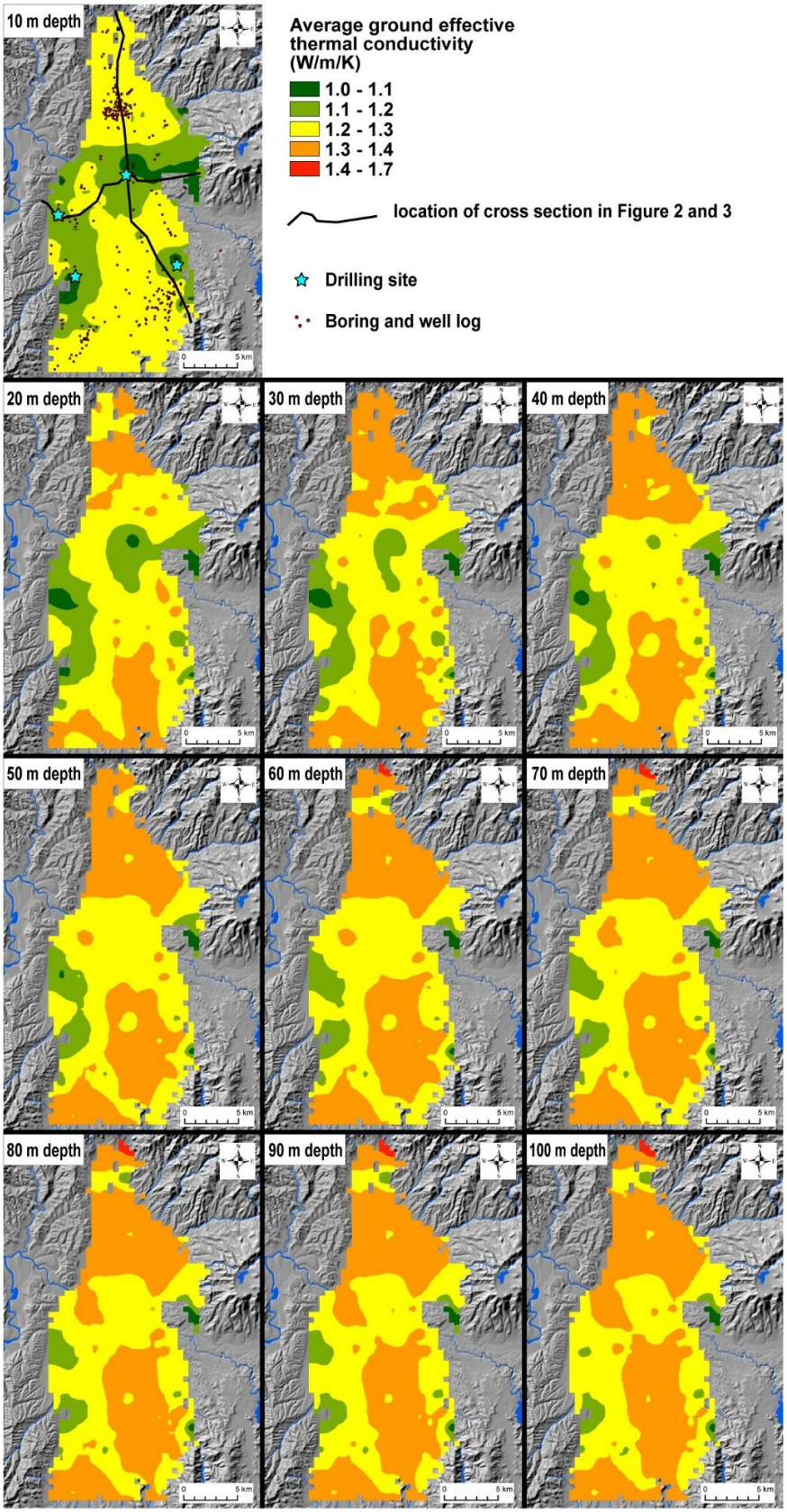


**Figure 6.** Distribution map of the average ground thermal conductivity from −10 m to −100 m depth. The relief map and elevation contour lines are drawn from the 50 m grid digital elevation map of the Geospatial Information Authority of Japan (GSI).

## 6. Discussion

Values of the average ground effective thermal conductivity were found to be higher in the northern and southern area of the Aizu Basin (Figure 6). The reconstructed shallow subsurface geological structure of the basin shows that the ratio of gravel layer is over 80% and intercalated mud beds tend to be thin and exist less continuously in these areas (Figures 3 and 5a). Moreover, the northern and southern basin areas correspond to an alluvial fan region with steeper surface gradients, which indicated the existence of preferable aquifers with higher groundwater flow velocities. Therefore, the higher apparent thermal conductivities in these areas are, therefore, expected due to heat advection by groundwater flow. In this paper, the apparent thermal conductivity is indicative of effective thermal conductivity when considering heat advection by groundwater flow.

The information of geological structure and ground effective thermal conductivity indicates that conventional closed-loop systems are feasible in the northern and southern basin areas including Kitakata and Aizu-Wakamatsu cities and Aizu-Misato Town. Groundwater flow velocity is expected to be higher in these areas due to a higher surface gradient and permeable layers. Shrestha et al. [11] also computed groundwater velocities in the Aizu Basin from the groundwater flow and heat transport analysis model and showed that the conventional closed-loop system was suitable in the northern and southern basin areas because of preferable geology and larger hydraulic gradients. The GHE depths of conventional systems are, therefore, suggested to be shorter because of higher apparent thermal conductivity.

Yet, relatively lower values of average ground effective thermal conductivity are estimated for the central and western floodplain areas except along the Aga River due to thick mud layers in the shallow subsurface (Figure 6). The average ground thermal conductivity slightly increased with depth in the central area due to an increase of the ratio of gravel layers below approximately 50 m depth (Figures 3 and 4). In contrast, the average ground thermal conductivity remains low in the western area up to 100 m depth because thick mud layers still lie in the deeper depth (Figure 4). The presence of these mud layers and a moderate surface gradient suggests the lower groundwater flow velocities in these floodplain areas. If a conventional closed-loop GSHP system will be installed in the central or western area (e.g., Shiokawa and Aizu-Bange towns), the GHE depth of the system is suggested to be longer (i.e., higher initial cost) than the GHE depth in the northern and southern areas. Shrestha et al. [11] also showed that heat exchange rates for the conventional closed-loop system were lower in the central area due to lower groundwater flow velocities computed from the analytical model. Instead, the occurrence of groundwater upflow forms artesian zones in the central and western basin areas and thick mud layers act as a confining layer [10,11]. Shrestha et al. [11] proposed that an alternative GSHP system to the conventional system using an artesian well is suitable for installation in the central basin area with groundwater upflow. Geological cross-sections may be helpful for surveying the artesian aquifers and confining mud layers. For example, Figure 2 indicates that thick mud layers occur widely around Aizu-Bange and play a role in the preferable confining layer with a higher artesian potential while the few mud layer zones along the Aga River may have a lower artesian potential.

Relatively lower than average ground effective thermal conductivity is also found in the eastern margin of the basin where tuff layers underlie at a shallow depth (Figures 3 and 6). Tuff layers have lower thermal conductivities as well as mud layers (Table 1), but their presence is almost negligible because of their deep distribution at >100 m depth throughout the basin except for the eastern margin area. In the eastern part of the Aizu-Wakamatsu City, which is the most populated district in the basin, several boring data show that thick tuff layers underlie gravel sediments of alluvial fans at a shallow depth (Figure 3). The three-dimensional structure of tuff layers around Aizu-Wakamatsu, however, remains unclear. The acquisition of geological and/or thermal data (e.g., performing a thermal response test) may be required for optimal planning of GSHP systems in this area.

Distribution maps of the average ground effective thermal conductivity should be available for municipalities to consider whether to adopt the installation of GSHP systems in the initial stage. Additionally, for municipalities such as Kitakata City, which has promoted the use of GSHP systems,

geological structure information is helpful for planning the system design as well as maps of the ground effective thermal conductivity. In regions with higher groundwater velocity, however, the apparent thermal conductivity should be higher than the ground effective thermal conductivity. In such regions, thermal response tests and/or evaluation of the suitability of GSHP systems based on 3D-groundwater flow and heat transport analysis are required. Geological and ground effective thermal conductivity data are also available as a reference for such an analysis.

## 7. Conclusions

This study assessed the installation potential of conventional closed-loop GSHP systems in the Aizu Basin in Northeast Japan based on its ground condition. The shallow subsurface geology, up to ca. 100 m in depth, was first analyzed and geological cross-sections were generated using data from the analysis of four sedimentary cores and lithofacies data of boring and snow melting well logs. The average ground effective thermal conductivity values of each log were calculated by length-weighted average methods and their distribution maps of depths from 10 m to 100 m were drawn.

The average ground effective thermal conductivity values were found to be higher in the northern and southern basin areas, 1.3–1.4 W/m/K, where gravel layers largely dominate and thin mud layers are scatted in various depths. These areas roughly correspond to alluvial fan regions with steep surface gradients, which points toward the existence of fine aquifers with higher groundwater flow velocities. Therefore, the average ground effective thermal conductivities in these areas may be expected to increase due to heat advection by groundwater flow. Yet, lower average ground effective thermal conductivity of 1.0–1.3 W/m/K were estimated in the central and western basin areas because of thick and well continuous mud layers in the shallow subsurface. Core analyses indicate that these mud layers spread widely in the central floodplain areas. The presence of these mud layers and moderate surface gradient indicate the lower groundwater flow velocities in these areas.

These thermal regimes based on the ground condition indicate that conventional closed-loop systems are more relevant in northern and southern areas than in central and western areas. This result correlates well with the assessment of the installation potential of conventional systems based on groundwater condition [11]. Instead, in the central and western areas, artesian zones formed due to the occurrence of groundwater upflow and thick mud layers acting as a confining layer [9]. An alternative GSHP system to the conventional closed-loop system using an artesian well is suitable for the installation in the central basin area with a groundwater upflow [10,11].

In this way, this study showed that the installation suitability of GSHP systems can be simply assessed using the information of a ground condition. The approach of the assessment using depth-based distribution maps of average ground thermal conductivity is unique in this study. The combination of geological cross-sections to the distribution maps may be helpful for considering the system design such as GHE depth and for surveying artesian aquifers and confining mud layers. Although this study is a regional case and a common conclusion cannot be shown due to different geological structure, the approach of this study is proper and valuable for the simple assessment of GSHP system installation in other sedimentary plains and basins with heterogeneous geology in Japan and other countries.

**Author Contributions:** T.I. is the principal investigator who prepared this manuscript. G.S. and S.K. contributed and advised on the calculation of ground effective thermal conductivity. Y.U. advised on the groundwater system. All authors approved the manuscript.

**Funding:** This research received no external funding.

**Acknowledgments:** The authors would like to thank the Kitakata Building Office and the Wakamatsu Building Office, Fukushima Prefecture for providing snow-melting well logs. We are also grateful to the reviewers for their valuable comments. We thank Esther Posner, PhD, from Edanz Group (www.edanzediting.com/ac) for editing a draft of this manuscript.

**Conflicts of Interest:** The authors declare no conflict of interest.

## Nomenclature

| | |
|---|---|
| GHE | Ground heat exchanger |
| GSHP | Ground-source heat pump |
| 3D | three-dimensional |
| $e$ | porosity |
| $L_k$ | total thickness of each geological facies |
| S | moisture saturation |
| $\lambda_a$ | thermal conductivity of air [W/m/K] |
| $\lambda_{ave}$ | average ground effective thermal conductivity [W/m/K] |
| $\lambda_f$ | thermal conductivity of fluid [W/m/K] |
| $\lambda_g$ | ground effective thermal conductivity [W/m/K] |
| $\lambda_s$ | thermal conductivity of solid (geological facies) [W/m/K] |

## References


1. Fujii, H.; Inatomi, T.; Itoi, R.; Uchida, Y. Development of suitability maps for ground-coupled heat pump systems using groundwater and heat transport modeling. *Geothermics* **2007**, *36*, 459–472. [CrossRef]
2. Omer, A.M. Ground-source heat pumps systems and applications. *Renew. Sustain. Energy Rev.* **2008**, *12*, 344–371. [CrossRef]
3. Lund, J.W.; Boyd, T.L. Direct utilization of geothermal energy 2015 worldwide review. *Geothermics* **2016**, *60*, 66–93. [CrossRef]
4. Ministry of Environment, Japan. Results of a Survey on the Use of Ground-Source Heat Pump Systems in Fiscal Year 2016. 2017. Available online: http://www.env.go.jp/press/103827 (accessed on 1 May 2018). (In Japanese)
5. Uchida, Y.; Yoda, Y.; Fujii, H.; Miyamoto, S.; Yoshioka, M. Adoption of suitability area for ground-coupled heat pump systems 1st paper, Development of suitability maps for ground-coupled heat pump systems using groundwater flow/heat transport modeling and geographic information system. *J. Geotherm. Res. Soc. Jpn.* **2010**, *32*, 229–239. (In Japanese with English Abstract)
6. Fujii, H.; Okubo, H.; Nishi, K.; Itoi, R.; Ohyama, K.; Shibata, K. An improved thermal response test for U-tube ground heat exchanger based on optimal fiber thermometers. *Geothermics* **2009**, *38*, 399–406. [CrossRef]
7. Yoshioka, M.; Uchida, Y.; Yoda, Y.; Fujii, H.; Miyamoto, S. Adoption of suitability area for ground-coupled heat pump systems 2nd paper, Development of heat exchange rate maps using groundwater flow/heat transport modeling. *J. Geotherm. Res. Soc. Jpn.* **2010**, *32*, 241–251. (In Japanese with English Abstract)
8. Nomoto, T.; Fujii, H.; Uchida, Y.; Kagabu, M.; Shimada, J. Application of geothermal heat pump systems in the warm areas from an aspect of the effect of a countermeasure against global warming. *J. Geotherm. Res. Soc. Jpn.* **2012**, *34*, 185–197. (In Japanese with English Abstract)
9. Shrestha, G.; Uchida, Y.; Yoshioka, M.; Fujii, H.; Ioka, S. Assessment of development potential of ground-coupled heat pump system in Tsugaru Plain, Japan. *Renew. Energy* **2015**, *76*, 249–257. [CrossRef]
10. Shrestha, G.; Uchida, Y.; Kuronuma, S.; Yamaya, M.; Katsuragi, M.; Kaneko, S.; Shibasaki, N.; Yoshioka, M. Performance evaluation of a ground-source heat pump system utilizing a flowing well and estimation of suitable areas for its installation in Aizu Basin, Japan. *Hydrogeol. J.* **2017**, *25*, 1437–1450. [CrossRef]
11. Shrestha, G.; Uchida, Y.; Ishihara, T.; Kaneko, S.; Kuronuma, S. Assessment of the installation potential of a ground source heat pump system based on the groundwater condition in the Aizu Basin, Japan. *Energies* **2018**, *11*, 1178. [CrossRef]
12. Hamada, Y.; Tanaka, S.; Nagano, K.; Tamura, H.; Takigawa, I.; Nakamura, Y.; Marutani, K.; Takashimizu, Y.; Takada, M. Feasibility study of underground thermal energy system by using digital national land information. *Trans. Soc. Heat. Air-Cond. Sanit. Eng. Jpn.* **2009**, *34*, 1–10. (In Japanese with English Abstract)
13. Takemura, T.; Nakazato, K.; Tajima, T.; Takano, Y. Extraction of geological conditions for ground heat utilization and the development of an independent source system utilizing heat and water power. *Proc. Inst. Nat. Sci. Nihon Univ.* **2014**, *49*, 155–162. (In Japanese with English Abstract)
14. Sakata, Y.; Katsura, T.; Nagano, K. A study on estimation of ground effective thermal conductivity as probability-weighted average. *J. Geotherm. Res. Soc. Jpn.* **2018**, *40*, 33–44. (In Japanese with English Abstract)

15. Hamamoto, H.; Shiraishi, H.; Hachinohe, S.; Ishiyama, T.; Satake, K.; Miyakoshi, A. Synthesis of subsurface temperature information and evaluation of potential for setting up ground heat exchangers in Saitama prefecture. *Butsuri-Tansa (Geophys. Explor.)* **2014**, *67*, 107–119. (In Japanese with English Abstract) [CrossRef]
16. Japan Meteorological Agency. Average Values of Meteorological Data in Wakamatsu. Available online: https://www.data.jma.go.jp/obd/stats/etrn/view/nml_sfc_ym.php?prec_no=36&block_no=47570&year=&month=&day=&view=p1 (accessed on 13 July 2018). (In Japanese)
17. Aizu-Wakamatsu City. Environmental Basic Plan in Second Phase. 2014. Available online: https://www.city.aizuwakamatsu.fukushima.jp/docs/2007121100044/files/keikakuhonnpenn.pdf (accessed on 19 July 2018). (In Japanese)
18. Kitakata City. Renewable Energy Vision (2017–2016) in Kitakata City. 2018. Available online: https://www.city.kitakata.fukushima.jp/uploaded/attachment/12510.pdf (accessed on 19 July 2018). (In Japanese)
19. Ikeda, T.; Imaizumi, T.; Togo, M.; Hirakawa, K.; Miyauchi, T.; Sato, H. *Atlas of Quaternary Thrust Faults in Japan*; University of Tokyo Press: Tokyo, Japan, 2002. (In Japanese)
20. Geological Survey of Japan, AIST. Seamless Digital Geological Map of Japan (1:200,000). 2015. Available online: https://gbank.gsj.jp/seamless/index_en.html (accessed on 1 May 2018).
21. Suzuki, K.; Manabe, K.; Yoshida, T. The late Cenozoic stratigraphy and geologic development of the Aizu Basin, Fukushima Prefecture, Japan. *Mem. Geol. Soc. Jpn.* **1977**, *14*, 17–44. (In Japanese with English Abstract)
22. Yamamoto, T.; Yoshioka, T. *Geology of the Wakamatsu District. With Geological Sheet Map at 1:50,000*; Geological Survey of Japan: Tsukuba, Japan, 1992; (In Japanese with English abstract).
23. Yamamoto, T.; Yoshioka, T; Makino, M.; Sumita, T. *Geology of the Kitakata District. Quadrangle Series, 1:50,000*; Geological Survey of Japan, AIST: Tsukuba, Japan, 2006; (In Japanese with English abstract).
24. Kaneko, R.; Nakagawa, S. Water balance in Aizu Basin. *Bull. Natl. Res. Inst. Agric. Eng. Jpn.* **1969**, *7*, 33–51. (In Japanese with English Abstract)
25. Kaneko, S.; Shibasaki, N.; Shoji, M.; Uchida, Y. Characteristics of changes in groundwater level and groundwater temperature based on long-term monitoring in the Aizu Basin, Fukushima, Japan. *Bull. Geol. Surv. Jpn.* **2016**, *67*, 183–208. (In Japanese with English Abstract) [CrossRef]
26. Akimoto, T.; Suzuki, Y. Water quality of confined groundwater in the Aizu Basin, Fukushima Prefecture. *Jpn. Assoc. Hydrol. Sci.* **1988**, *18*, 14–21. (In Japanese with English Abstract)
27. Ishihara, T.; Suzuki, T.; Hongo, M.; Uchida, Y. Study of shallow subsurface geology based on analysis of sedimentary cores drilled in the Aizu Basin, Northeast Japan. Presented at the Japan Geoscience Union and American Geophysical Union Meeting, Chiba, Japan, 20–25 May 2017.
28. Suzuki, T.; Saito, H.; Kasahara, A.; Kuriyama, E.; Imaizumi, T. Late Quaternary tephrostratigraphy of underground sediments in the middle west part of Aizu Basin, Fukushima, northeast Japan. *Quat. Res. (Daiyonki-Kenkyu)* **2016**, *55*, 1–16. (In Japanese with English Abstract) [CrossRef]
29. Ishihara, T.; Suzuki, T.; Hongo, M.; Uchida, Y. Geological stratigraphy of a drilling core based on analysis of tephras and pollen assemblages in the western part of Aizu Basin, Northeast Japan. Presented at the Japan Geoscience Union Meeting, Chiba, Japan, 20–24 May 2018.
30. Diersch, H.J.G. *FEFLOW Reference Manual*; WASY GmbH Institute for Water Resources Planning and Systems Research: Berlin, Germany, 2005.
31. Diersch, H.J.G. *FEFLOW: Finite Element Modeling of Flow, Mass and Heat Transport in Porous and Fractured Media*; Springer: Berlin, Germany, 2014.
32. Ghanbarian, B.; Daigle, H. Thermal conductivity in porous media: Percolation-based effective-medium approximation. *Water Resour. Res.* **2015**, *52*, 295–314. [CrossRef]